ORIGINAL ARTICLE – CANCER RESEARCH

Combination of Cl-IB-MECA with paclitaxel is a highly effective cytotoxic therapy causing mTOR-dependent autophagy and mitotic catastrophe on human melanoma cells

Ana S. Soares · Vera M. Costa · Carmen Diniz ·
Paula Fresco

Abstract

Purpose Metastatic melanoma is the deadliest form of skin cancer. It is highly resistant to conventional therapies, particularly to drugs that cause apoptosis as the main anti-cancer mechanism. Recently, induction of autophagic cell death is emerging as a novel therapeutic target for apoptotic-resistant cancers. We aimed to investigate the underlying mechanisms elicited by the cytotoxic combination of 2-chloro-N(6)-(3-iodobenzyl)-adenosine-5′-N-methyl-uronamide (Cl-IB-MECA, a selective A_3 adenosine receptor agonist; 10 µM) and paclitaxel (10 ng/mL) on human C32 and A375 melanoma cell lines.

Methods Cytotoxicity was evaluated using 3-(4,5-dimethylthiazol-2-yl)-2,5-diphenyl tetrazolium bromide reduction, neutral red uptake, and lactate dehydrogenase leakage assays, after 48-h incubation. Autophagosome and autolysosome formation was detected by fluorescence through monodansylcadaverine-staining and CellLight® Lysosomes-RFP-labelling, respectively. Cell nuclei were visualized by Hoechst staining, while levels of p62 were determined by an ELISA kit. Levels of mammalian target of rapamycin (mTOR) and the alterations of microtubule networks were evaluated by immunofluorescence.

Results We demonstrated, for the first time, that the combination of Cl-IB-MECA with paclitaxel significantly increases cytotoxicity, with apoptosis and autophagy the major mechanisms involved in cell death. Induction of autophagy, using clinically relevant doses, was confirmed by visualization of autophagosome and autolysosome formation, and downregulation of mTOR and p62 levels. Caspase-dependent and caspase-independent mitotic catastrophe evidencing micro- and multinucleation was also observed in cells exposed to our combination.

Conclusions The combination of Cl-IB-MECA and paclitaxel causes significant cytotoxicity on two melanoma cell lines through multiple mechanisms of cell death. This multifactorial hit makes this therapy very promising as it will help to avoid melanoma multiresistance to chemotherapy and therefore potentially improve its treatment.

Keywords Melanoma · Autophagy · mTOR · Apoptosis · Mitotic catastrophe

A. S. Soares · C. Diniz · P. Fresco
REQUIMTE/Laboratório de Farmacologia, Departamento de Ciências do Medicamento, Faculdade de Farmácia, Universidade do Porto, Porto, Portugal

V. M. Costa
REQUIMTE/Laboratório de Toxicologia, Departamento de Ciências Biológicas, Faculdade de Farmácia, Universidade do Porto, Porto, Portugal

P. Fresco (✉)
Departamento de Farmacologia, Faculdade de Farmácia, Universidade do Porto, Rua de Jorge Viterbo Ferreira, 228, 4050-313 Porto, Portugal
e-mail: pfresco@ff.up.pt

Abbreviations

Ac-DEVD-CHO	N-Ac-Asp-Glu-Val-Asp-CHO
Cl-IB-MECA	2-Chloro-N(6)-(3-iodobenzyl)-adenosine-5′-N-methyl-uronamide
CTR	Control
DMSO	Dimethyl sulfoxide
DMEM-HG	Dulbecco's modified Eagle's medium—high glucose
FBS	Foetal bovine serum
LAMP1	Lysosomal-associated membrane protein 1
LDH	Lactate dehydrogenase

LY294002	2-(4-Morpholinyl)-8-phenyl-4*H*-1-ben-zopyran-4-one hydrochloride
3-MA	3-Methyladenine
MC	Mitotic catastrophe
MDC	Monodansylcadaverine
mTOR	Mammalian target of rapamycin
MTT	3-(4,5-Dimethylthiazol-2-yl)-2,5-diphe-nyl tetrazolium bromide
NAC	*N*-acetylcysteine
NR	Neutral red
PI3K	Phosphoinositide 3-kinase
PXT	Paclitaxel
RFP	Red fluorescent protein
ROS	Reactive oxygen species
SQSTM1	Sequestosome 1

Introduction

Metastatic melanoma is the deadliest form of skin cancer, and its incidence is globally rising (Jemal et al. 2010). This aggressive disease has an extremely poor prognosis because it is highly resistant to conventional therapies (Tawbi and Kirkwood 2007). The overall survival of patients with metastatic melanoma is lower than 2 years (Jemal et al. 2010). Indeed, it is the most treatment-resistant human cancer (de Souza et al. 2012), remaining one of the greatest challenges in oncotherapy.

Most chemotherapeutic drugs are described to cause cell death through apoptosis (Fulda and Debatin 2006). Apoptosis is a highly structured and orchestrated cell suicide mechanism induced by physiological or pathological stimuli and controlled by specific genes and multiple signalling pathways (Elmore 2007). Activation of caspase-dependent and/or caspase-independent processes results in apoptosis that include features of cell shrinkage, nuclear fragmentation, chromatin condensation, and membrane blebbing (Hengartner 2000).

Recently, increasing evidence revealed that some chemotherapeutic drugs can also act by inducing mitotic catastrophe (MC), which is characterized by micro- and multinucleated cells, resulting in cell death (Hanahan and Weinberg 2011; Vakifahmetoglu et al. 2008). It is being reported that MC shares several biochemical hallmarks with apoptosis, in particular caspase activation, being proposed as a special case of apoptosis (Castedo et al. 2004b). However, it is not yet well established whether MC results in death that requires caspase activation or not (Mansilla et al. 2006), and the clear definition of the concepts of MC is still missing (Vakifahmetoglu et al. 2008). Nevertheless, induction of MC is an attractive strategy for developing new anticancer therapies (Hung et al. 2013).

It is well accepted that the limited success of most current therapeutic strategies used in metastatic melanoma is due, at least in part, to cancer cells ability in escaping apoptosis, thus leading to drug resistance (Soengas and Lowe 2003). Drugs that activate pathways overcoming melanoma's apoptosis resistance and inducing cell death have, therefore, great potential for melanoma therapeutic interventions. Recently, another type of cell death, autophagy, has become an alternative approach to anticancer therapy (Hanahan and Weinberg 2011), as pro-autophagic drugs seem to represent a novel therapeutic weapon for apoptosis-resistant cancers (Tsujimoto and Shimizu 2005).

Autophagy is mainly a self-destructive process that degrades intracellular structures in response to stress, contributing for both cell survival, in adverse conditions (nutrient starvation or metabolic stress), and conversely cell death (White and DiPaola 2009). This process begins with the sequestration of cytoplasmic material (cargo) in double-membrane vacuoles called autophagosomes or autophagic vacuoles, which undergo maturation, including fusion with lysosomes to form autolysosomes, where the cargo is degraded (Kung et al. 2011).

The AKT/mammalian target of rapamycin (mTOR) signalling pathway promotes tumour cell proliferation and resistance to drug-induced apoptosis (LoPiccolo et al. 2008), being highly active in several cancers including melanoma (Dai et al. 2005). This pathway is also a key negative regulator of autophagy (Jung et al. 2010). In fact, several studies have reported the importance of phosphoinositide 3-kinase (PI3K)/AKT/mTOR pathway in regulating autophagy (Jung et al. 2010; Saiki et al. 2011), although, at this point, little is known in cancer regulation. Class I and class III PI3K regulate autophagy differently: class I PI3K/AKT/mTOR pathway inhibits autophagy and class III PI3K, by contrast, promotes the sequestration of cytoplasmic material that occurs during autophagy, at the trans-Golgi network (Liu et al. 2013; Kihara et al. 2001). Currently, it has been proposed that the use of PI3K/AKT/mTOR pathway inhibitors may be a successful strategy to treat melanoma (Gao et al. 2013).

Evidence suggests that tumour cells can undergo both apoptosis and autophagic cell death in response to therapy because these pathways might be triggered by the same signal (Maiuri et al. 2007). However, the precise crosstalk regarding the relation between these two cell death mechanisms is complex and sometimes contradictory (Shen et al. 2011). Therefore, understanding the mechanisms underlying apoptosis–autophagy interaction is crucial for the development of therapeutic strategies to improve the efficacy of anticancer agents.

Recently, we provided evidence that simultaneous treatment with Cl-IB-MECA (2-chloro-*N*(6)-(3-iodobenzyl)-adenosine-5′-*N*-methyl-uronamide, a selective A_3 adenosine receptor agonist) and paclitaxel (PXT) potentiates human C32 melanoma cells cytotoxicity, mainly through

apoptotic pathways (Soares et al. 2013), however, through A_3 adenosine receptor-independent mechanisms. The combination revealed a good potential on melanoma treatment since it allows PTX doses reduction and consequently the decrease in adverse effects and multiresistance recurrence in melanoma. However, in this previous work, not all cytotoxicity induced by Cl-IB-MECA and PXT combinations could be explained just by apoptosis-mediated cell death. In the present work, efforts were made in order to elucidate the possible involvement of other cell death pathways, namely autophagy. To address this question, we investigated the cytotoxic effects induced by Cl-IB-MECA (10 μM) and PXT (10 ng/mL), alone or in combination, on two human melanoma cell lines (C32 and A375 cells) as to increase knowledge on this potentially useful anticancer therapeutic strategy.

Materials and methods

Chemicals

All reagents used were of analytical grade. Cl-IB-MECA and 3-methyladenine (3-MA) were obtained from Tocris Bioscience (Bristol, UK). Lactate dehydrogenase (LDH) assay kit was purchased from Promega Bioscience (VWR, Porto, Portugal). Caspase inhibitor (*N*-Ac-Asp-Glu-Val-Asp-CHO, Ac-DEVD-CHO) was purchased from Calbiochem (Millipore, Interface, Amadora, Portugal). Sequestosome 1(SQSTM1)/p62 ELISA kit was purchased to Cell Signaling Technology (Izasa, Lisboa, Portugal). Bio-Rad RC DC protein assay kit was purchased to Biorad (Amadora, Portugal). Foetal bovine serum (FBS), Glutamax, trypsin/EDTA, Alexa Fluor® 594 (anti-mouse), Alexa Fluor® 568 (anti-goat) and CellLight® Lysosomes-RFP-BacMam 2.0 were obtained from Invitrogen (Alfagene, Carcavelos, Portugal). Goat anti-mTOR antibody was purchased to Santa Cruz Biotechnology (Reagente 5, Porto, Portugal). Dulbecco's modified Eagle's medium-high glucose (DMEM-HG), penicillin/streptomycin (10 000 U/mL), PXT, LY294002, 3-(4,5-dimethylthiazol-2-yl)-2,5-diphenyl tetrazolium bromide (MTT), neutral red (NR), monodansylcadaverine (MDC), Hoechst 33258, mouse anti-α-tubulin antibody, dimethyl sulfoxide (DMSO), *N*-acetylcysteine (NAC), and all other chemicals were purchased from Sigma-Aldrich (Sigma-Aldrich-Química SA, Sintra, Portugal) of the highest purity available.

Cell culture

Human C32 and A375 metastatic melanoma cells obtained from ECACC to SIGMA (Sigma-Aldrich-Química SA, Sintra, Portugal) were used in this study. Cells were seeded in DMEM-HG medium with 10 % of FBS, 1 % of a mixture of penicillin/streptomycin and 1 % of Glutamax, pH 7.4. Cells were incubated at 37 °C in a humidified atmosphere (95 % air; 5 % CO_2). For cell culture maintenance, cells were grown in monolayer and sub-cultivated twice a week. Cell passaging was done by trypsinization. All experiments were carried out with cells at 70–80 % confluence and from batches with passage numbers lower than 50.

Cell treatment

Cells were prepared using an initial cell density of 3.0×10^4 cells/cm² (A375 cells) and 5.0×10^4 cells/cm² (C32 cells), and allowed to attach for 24 h. Cells were then treated with Cl-IB-MECA [10 μM (Soares et al. 2013)] and/or PXT [10 ng/mL (Soares et al. 2013)] for 24 or 48 h. When the class III PI3K inhibitor, 3-MA [2.5 mM (Santoni et al. 2013)], and/or the caspase inhibitor, Ac-DEVD-CHO [50 μM (Soares et al. 2013)], were used to prevent autophagy and/or apoptosis, respectively, they were added 1 h prior to the addition of other compounds. The antioxidant NAC [1 mM (Martins et al. 2013)], when used, was also added 1 h prior to the addition of Cl-IB-MECA and/or PXT. During all the experimental period, cells were maintained at 37 °C with 5 % CO_2.

Cytotoxicity assays

Cells were seeded in 96-well plates and treated as in section *Cell treatment*. Vehicle (cells exposed to DMSO at maximum final concentration of 0.1 % v/v) and blank (without cells) wells were also incubated at 37 °C, for 48 h. Treatments, vehicle, and blank conditions were performed in triplicate, initiated, and processed in parallel.

MTT reduction assay

Mitochondrial function was evaluated as an index of cell cytotoxicity, since mitochondrial dehydrogenases of living cells can reduce the MTT (yellow) to formazans (Mosmann 1983). At the end of the treatment incubation period (48 h), cells were processed as previously described by our group (Soares et al. 2013).

NR uptake assay

Lysosomal functionality was spectrophotometrically evaluated and represented as the percentage of NR dye incorporated in the cells. This dye easily penetrates viable cells and accumulates intracellularly in lysosomes (Repetto et al. 2008). At the end of treatment incubation period (48 h), cells were processed as already described by us (Soares et al. 2013). Cells labelled with NR were also analysed by an AE2000 Motic® inverted microscope coupled to a

Moticam 5 digital camera (Spectra Services, VWR International, Carnaxide, Portugal). Images from six random fields/well were captured (magnification of 400×).

LDH leakage

Cell death (measurement of membrane integrity evaluated by the percentage of LDH released over total LDH) was assessed using a LDH assay kit according to the manufacturer's instructions. At the end of the treatment incubation period (48 h), cells were processed as previously described (Soares et al. 2013).

Autophagosome and lysosome staining

Cells were seeded in chamber slide systems and treated according to section *Cell treatment*. The PI3K (class I) inhibitor, LY294002 [50 µM (Xing et al. 2008)], was used as a positive control for autophagy. Lysosomal morphology was evaluated after the addition of a lysosomal associated membrane protein 1-red fluorescent protein (LAMP1-RFP) fusion construct (CellLight® Lysosomes-RFP; 20 particles/cell), according to the manufacturer's instructions. After 48-h incubation with the compounds, media was removed and cells were incubated with 0.05 mM MDC (autofluorescent dye) in PBS at 37 °C for 10 min (protected from light) (Biederbick et al. 1995). Cells were then washed with PBS and analysed by a Nikon Eclipse E400 fluorescence microscope coupled to a digital camera (Nikon Digital Sight DS-5Mc, New Jersey, USA). Images from ten random fields *per* condition were captured (magnification of 1,000×). Merged images were obtained using Adobe Photoshop CS5 software. MDC-stained autophagosomes are displayed in green and LAMP1-stained lysosomes in red.

Determination of p62 levels

Cells were seeded in 6-well plates. Twenty-four hours after cell treatment (section *Cell treatment*), p62 levels were evaluated using the p62 ELISA kit, according to the manufacturer's instructions. The p62 levels were only assessed in the conditions where the MDC-stained autophagosomes were observed. LY294002 [50 µM (Xing et al. 2008)] was used as a positive control for autophagy. The levels of p62 were expressed as optic density (OD) *per* amount of protein.

Protein content determination

Protein content of cellular fractions, in total cell lysates, for p62 assays was determined using the Bio-Rad RC DC protein assay kit, in accordance with the manufacturer's instructions. Stock solutions of bovine serum albumin were used as standards.

Immunofluorescence assay

Cells were seeded in chamber slide systems and treated as in section *Cell treatment*. LY294002 [50 µM (Xing et al. 2008)] was used as a positive control for autophagy. After cell treatment, cells were washed with PBS and fixed in 4 % paraformaldehyde (10 min, room temperature). Cells were blocked and permeabilized with 1 % (v/v) FBS containing 0.25 % (v/v) Tween 20, for 30 min, at 4 °C. Next, cells were incubated with the primary antibodies, goat anti-mTOR (1:200), or mouse anti-α tubulin (1:500), depending on the experiment goal, overnight at 4 °C. After washing with PBS, cells were incubated with Hoechst 33258 (5 µg/mL) for 15 min and then incubated with the respective secondary antibodies, Alexa Fluor® 568 (1:1,500) or Alexa Fluor® 594 (1:1,000) for 1 h (room temperature, protected from light). Finally, slides were washed with PBS and mounted with PBS/glycerol solution (3:1). Cells were examined in a Nikon Eclipse E400 fluorescence microscope coupled to a digital camera (Nikon Digital Sight DS-5Mc, New Jersey, USA). Images from ten random fields *per* condition were captured (magnification of 1,000×). Merged images were obtained using Adobe Photoshop CS5 software. Depending on the experiment performed, Alexa Fluor® 568-stained mTOR and Alexa Fluor® 594-stained α-tubulin (microtubules) are displayed in red. Hoechst 33258-labelled nuclei are displayed in blue. Image processing for quantification of cell nuclei with typical morphologic mitotic catastrophe (MC) features (micro- and multinucleated cells) (Vakifahmetoglu et al. 2008) was done using ImageJ software. Ratios of MC and normal nuclei were obtained using images from ten random fields *per* condition (magnification of 400×).

Statistical analysis

Results are presented as mean ± SEM for *n* experiments. Statistical comparisons between groups were performed with one-way ANOVA, after Shapiro–Wilk test normality evaluation. Statistical significance was accepted at *p* values <0.05. The Student–Newman–Keuls post hoc test was used once a significant *p* was achieved.

Results

Cl-IB-MECA in combination with PXT causes cytotoxicity in human metastatic melanoma cells

Human C32 and A375 melanoma cells were treated with 10 µM of Cl-IB-MECA (Cl10), 10 ng/mL of PXT (PXT10), and the combination of the two (Cl10 + PXT10), for 48 h (Fig. 1).

Fig. 1 Cytotoxic effects elicited by Cl-IB-MECA (10 μM; Cl10) and/or PXT (10 ng/mL; PXT10) on human C32 (*white bars*) and A375 (*grey bars*) melanoma cells, after 48-h incubation. DMSO (final concentration of 0.1 % v/v) in DMEM-HG was used as vehicle. **a** Results of MTT reduction (% from vehicle) are presented as mean ± SEM, $n = 12$ of 4 independent experiments. Significant differences (one-way ANOVA test, followed by the Student–Newman–Keuls post hoc test): **$p < 0.01$ versus vehicle; ***$p < 0.001$ versus vehicle; ###$p < 0.001$ versus C32 cells for the same condition. **b** Results of NR uptake (% from vehicle) are presented as mean ± SEM, $n = 12$ of 4 independent experiments. Significant differences (one-way ANOVA test, followed by the Student–Newman–Keuls post hoc test): **$p < 0.01$ versus vehicle; ***$p < 0.001$ versus vehicle; ###$p < 0.001$ versus C32 cells for the same condition. **c** Representative photographs of C32 and A375 cells after NR staining. Scale bar, 10 μm
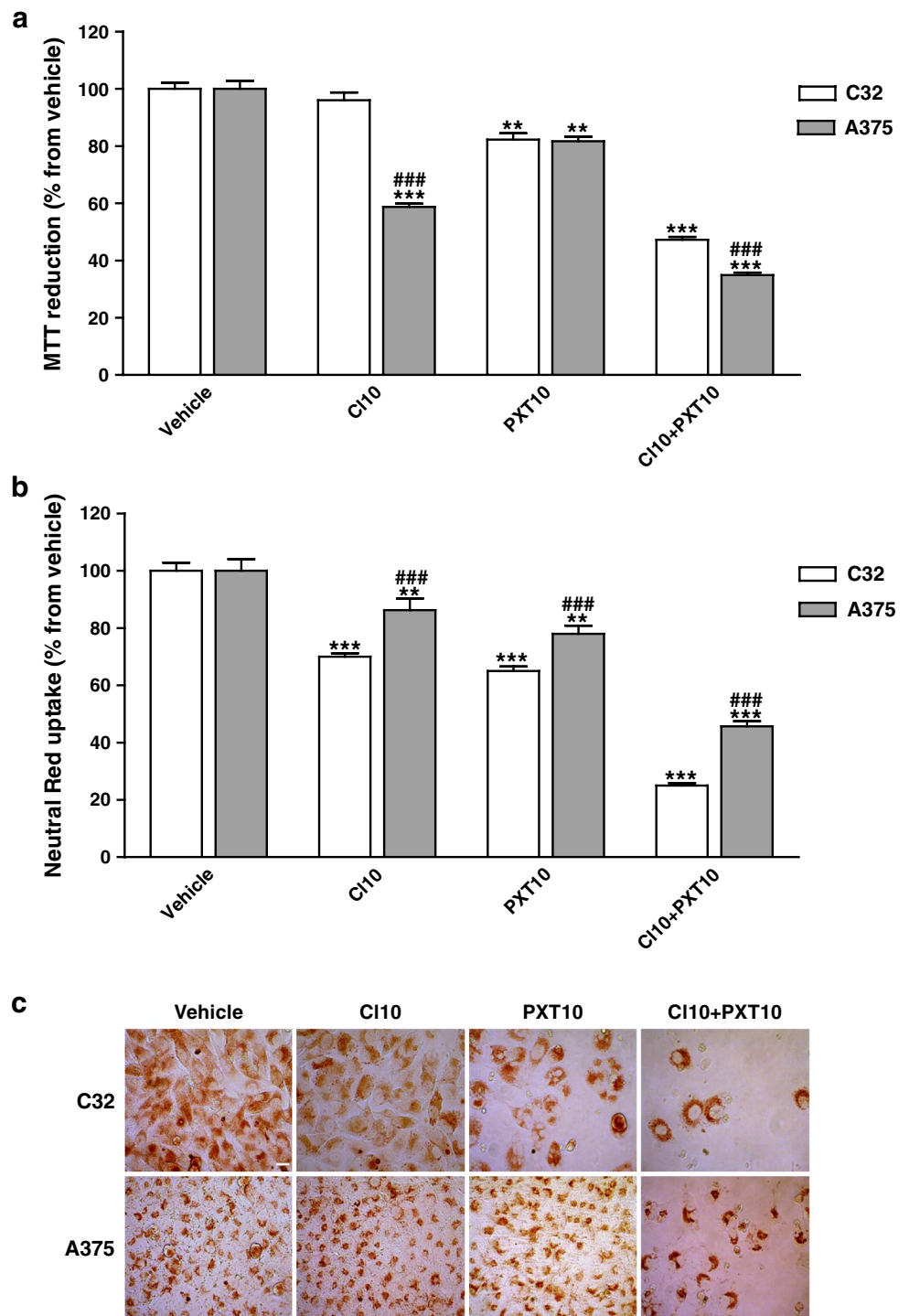
Results from the MTT reduction assay showed that mitochondrial function of cells incubated with Cl10 had different outcomes in C32 and A375 cells (Fig. 1a): No cytotoxicity was observed in C32 cells, whereas significant mitochondrial dysfunction occurred on A375 cells. However, both cell lines treated with PXT10 demonstrated a significant and similar decrease in mitochondrial activity (Fig. 1a). When combined, Cl10 and PXT10 (Cl10 + PXT10) caused a higher cytotoxicity in both cell lines, although more pronounced on A375 cells, comparatively to the effect caused by this treatment on C32 cells (Fig. 1a).

Active lysosomal uptake (NR uptake assay) was also evaluated in the conditions described above (Fig. 1b). Cl10

and PXT10 were able to reduce lysosomal NR uptake in both cell lines, although with a higher NR uptake impairment on C32 cells. Moreover, lysosomal uptake was clearly impaired when the combination of Cl10 with PXT10 (Cl10 + PXT10) was tested in both melanoma cell lines, when compared to the effects elicited by the individual compounds.

The cytotoxic effects observed with the NR uptake were also visualized (Fig. 1c). Images of A375 and, particularly, of C32 cells revealed that NR uptake was clearly compromised in all treatment groups when compared to the vehicle. In fact, especially in C32 cells, it is observable in Cl10 that although a similar number of cells *per* field is seen, NR uptake is clearly diminished. For both cell lines, the combination of drugs caused a significant decrease in the number of cells *per* field, whereas incubation of cells with individual compounds affects NR uptake without significantly compromising cells integrity (Fig. 1c).

Cell death elicited by the combination of Cl-IB-MECA and PXT is mediated by autophagy and apoptosis with dissimilar importance on C32 and A375 cells

To explore the role of autophagy and/or apoptosis in the cytotoxicity induced by Cl-IB-MECA (10 μM), PXT (10 ng/mL), the combination of both human C32 and A375 melanoma cells were incubated with these compounds, in the absence or in the presence of an autophagy inhibitor, 3-MA (2.5 mM) and/or a caspase inhibitor, Ac-DEVD-CHO (50 μM), as described in the Methods section. Cell death (LDH leakage assay) was assessed at 48 h (Fig. 2). Although Cl10 did not lead to C32 cell death (Fig. 2a), this effect was statistically significant on A375 cells (Fig. 2b). Moreover, pre-treatment of A375 cells with the caspase inhibitor (Ac-DEVD-CHO) did not prevent cell death, while the autophagy inhibitor (3-MA) completely blocked A375 cell death induced by Cl10. These data suggest that cytotoxicity caused by Cl10 in A375 cells is mediated only by autophagy (Fig. 2b).

Incubations of C32 and A375 cells with PXT10 induced significant cell death, when compared to vehicle. Furthermore, pre-incubation of cells with the caspase inhibitor (Ac-DEVD-CH) completely prevented cell death in both cell lines (Fig. 2), whereas 3-MA (autophagy inhibitor) had no effect upon the PXT10 cytotoxic effect. This result indicates that the cytotoxic effect induced by PXT10 in melanoma cells occurs through caspase-dependent apoptotic events.

Cell death was more pronounced when melanoma cells were treated simultaneously with Cl10 and PXT10 (Cl10 + PXT10), comparatively to vehicle and individual treatments at 48 h (Fig. 2). Moreover, the combination of drugs caused a higher increment of LDH leakage on C32

(Fig. 2a) than on A375 cells (Fig. 2b). Pre-treatment of C32 cells with the caspase inhibitor (Ac-DEVD-CHO) significantly attenuated cytotoxicity (Fig. 2a) but did not totally abrogate this effect, suggesting that apoptosis is not the only event involved in cytotoxicity occurring in C32 cells. Cells were also incubated with the combination of Cl10 and PXT10, after treatment with 3-MA, an autophagy inhibitor. This compound demonstrated to be more efficient in preventing LDH leakage than the caspase inhibitor, but total ablation of the cytotoxic effect was only achieved when C32 cells were pre-treated simultaneously with both inhibitors (Fig. 2a). These results suggest that Cl10 with PXT10 caused C32 cell death through activation of both autophagic and apoptotic events, with autophagy activation having the major role in cell death.

A375 cells were treated in the previously referred conditions and for the same incubation time (Fig. 2b). The caspase inhibitor (Ac-DEVD-CHO) or the autophagy inhibitor (3-MA) were only able to partially, and to a similar extent, prevent LDH leakage caused by Cl10 in combination with PXT10. Moreover, the mixture of inhibitors did not completely block the cytotoxic effect elicited by the combination of Cl10 and PXT10 (Fig. 2a). These results suggest that although autophagic and apoptotic cell deaths seem to contribute equally for the cytotoxic effect caused by Cl10 in combination with PXT10, these are not the only pathways involved, since total prevention of A375 cell death was not achieved (Fig. 2b).

Importantly, the simultaneous treatment with the two inhibitors did not cause any cellular cytotoxicity, indicating that autophagy and apoptosis are not constitutively activated in human C32 or A375 melanoma cells (Fig. 2).

Autophagosomes fusion with lysosomes is induced by Cl-IB-MECA on A375 cells and by the combination of Cl-IB-MECA with PXT on C32 and A375 cells

Human C32 and A375 melanoma cells were incubated with Cl-IB-MECA (10 μM, Cl10), PXT (10 ng/mL, PXT10), and the combination of both (Cl10 + PXT10), in the absence or in the presence of an autophagy inhibitor, 3-MA (2.5 mM), for 48 h, as described in the Methods section. LY294002 (50 μM) was used as a positive control for autophagy. Imaging of autophagosomes was done by using the fluorescent dye MDC and showed that, in C32 cells treated with Cl10 + PXT10, in A375 cells treated with Cl10 and Cl10 + PXt10 (conditions where there was prior indication of autophagy assessed by LDH assay, Fig. 2), and in both cell lines treated with the positive control of autophagy LY294002, autophagosomes appeared as green larger condensed structures (white arrows, Fig. 3). Similarly, the spatial distribution of lysosomes (Lyso-RFP) is altered after these treatments, showing larger red structures

Fig. 2 Cl-IB-MECA in combination with PXT caused melanoma cell death mediated by apoptosis and autophagy. **a** C32 and **b** A375 melanoma cells treated with Cl-IB-MECA (10 μM; Cl10) and/or PXT (10 ng/mL; PXT10), after 48-h incubation, in the absence (*white bars*) or in the presence of the caspase inhibitor, Ac-DEVD-CHO (50 μM; *hatched bars*), the autophagy inhibitor, 3-MA (2.5 mM, *grey bars*), or both (*black bars*). DMSO (final concentration of 0.1 % v/v) in DMEM-HG was used as vehicle. Results of LDH leakage (% of total LDH) are presented as mean ± SEM, $n = 12$ of 4 independent experiments. Significant differences (one-way ANOVA test, followed by the Student–Newman–Keuls post hoc test): *$p < 0.05$ versus vehicle; **$p < 0.01$ versus vehicle; ***$p < 0.001$ versus vehicle; ##$p < 0.01$ versus same condition with DMSO (0.1 % v/v); ###$p < 0.001$ versus same condition with DMSO (0.1 % v/v)
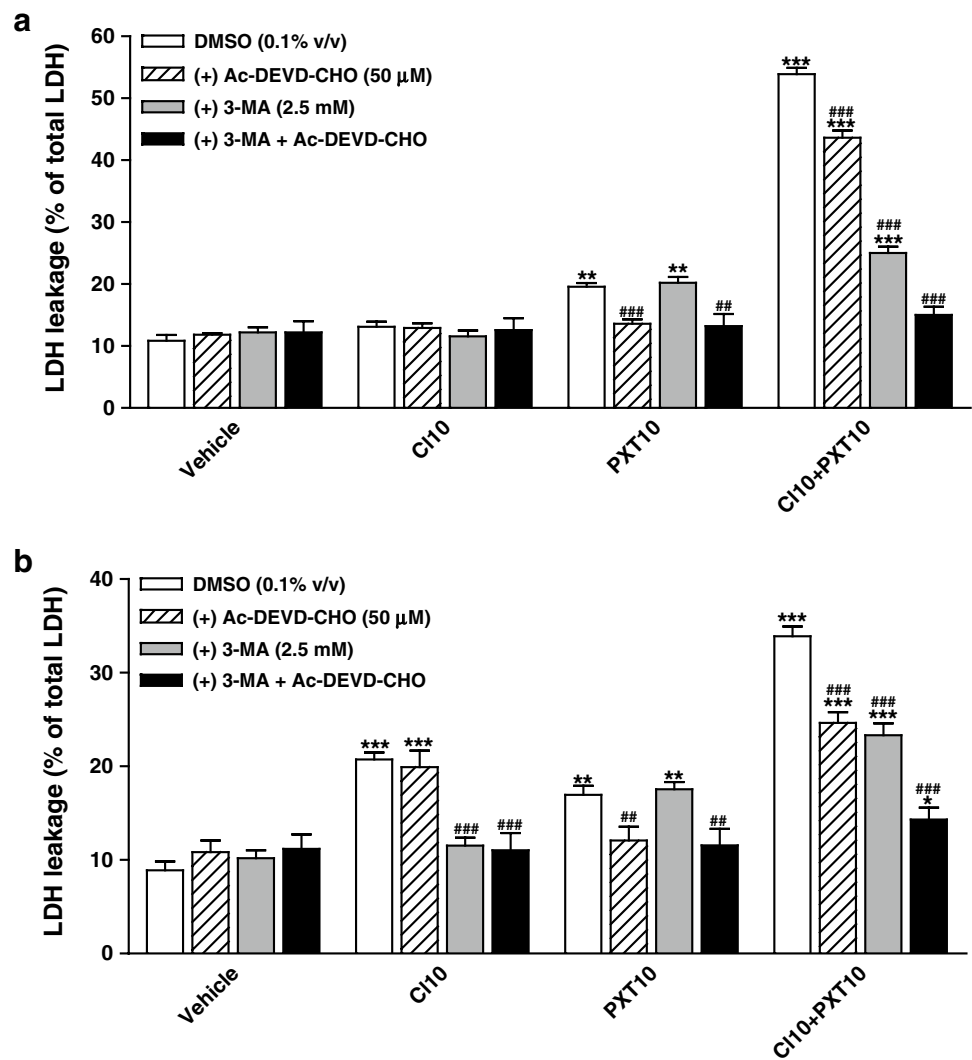
(white arrows, Fig. 3). Formation of autolysosomes, as a result of the fusion between autophagosomes with lysosomes, was confirmed by observation of co-localization of the structures in the above conditions (yellow structures in merged images, white arrows, Fig. 3).

On the contrary, in conditions where there was no indication of autophagy (Fig. 2), autophagosomes were visualized as small punctate scattered structures (dots). Moreover, in those conditions (vehicle, 3-MA, Cl10 and PXT10 for C32 cells; vehicle, 3-MA, PXT10 for A375), lysosome labelling was very tenuous and yellow structures (autolysosomes) were not observed on merged images (Fig. 3). These findings indicate that, in these cell treatments, the occurrence of autophagy can be discarded.

Images from cells pre-incubated with the autophagy inhibitor 3-MA, showed decreased MDC and lysosomal staining, suggesting that A375 cells treated with Cl10 and both lines treated with the combination Cl10 + PXT10 present autophagic cell death, to some extent.

p62 levels are decreased in Cl-IB-MECA-induced A375 autophagic cell death and in Cl-IB-MECA plus PXT-induced autophagic melanoma cell death in both cell lines

Considering the fact that p62 is rapidly degraded during autophagy, analysis of its intracellular levels was performed by an ELISA kit at 24 h, as to confirm the involvement of autophagic cell death in the conditions where autophagy is suspected to occur, based on the results obtained by LDH leakage and MDC staining assays. C32 cells were incubated with the combination of Cl10 with PXT10 (Cl10 + PXT10), and A375 cells with Cl10 and Cl10 + PXT10 in the absence or in the presence of an autophagy inhibitor, 3-MA (2.5 mM), for 24 h, as described in methods section. LY294002 (50 μM) was, once more, used as a positive control for autophagy.

C32 and A375 human melanoma cell lines have similar basal levels of p62 protein and cell treatments with
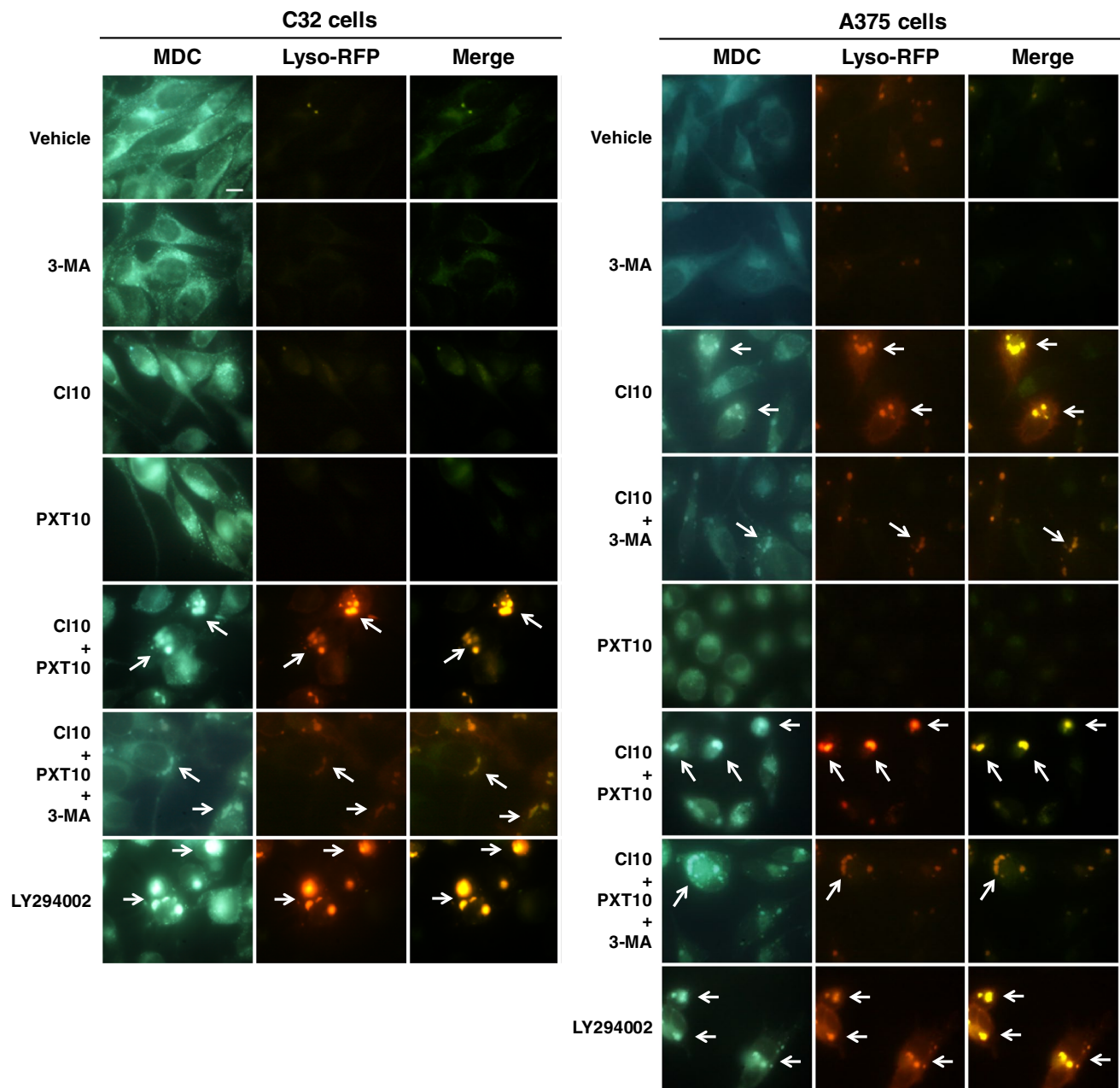
Fig. 3 Autophagosomes fusion with lysosomes induced by Cl-IB-MECA (10 μM; Cl10) and/or PXT (10 ng/mL; PXT10) on human C32 and A375 melanoma cells, after 48-h incubation, in the absence or in the presence of the autophagy inhibitor, 3-MA (2.5 mM). DMSO (final concentration of 0.1 % v/v) in DMEM-HG was used as vehicle and LY294002 (50 μM) as a positive control for autophagy.

Representative photographs of C32 and A375 cells after MDC (autophagosomes; *green*) and Lyso-RPF (lysosomes; *red*) staining ($n = 4$ independent experiments). Merged images indicate fusion of autophagosomes with lysosomes (*yellow*). Scale bar, 10 μm. *Arrows* indicate condensed autophagosomes (MDC) and lysosomes (Lyso-RPF) and intense autolysosomes formation (merge)

LY294002 resulted in significant reduction in p62 levels on both cell lines, after 24-h incubation (Fig. 4), as expected.

C32 cells present significant p62 protein levels reduction, after 24-h incubation with Cl10 + PXT10, when compared to the levels measured in cells treated with vehicle only (Fig. 4a). Moreover, the autophagy inhibitor (3-MA) was able to completely prevent this p62 degradation (Fig. 4a).

For A375 cells, treatment with Cl10 caused a significant decrease in p62 levels, being this effect more marked when cells were simultaneously treated with Cl10 and PXT10 (Fig. 4b). In this cell line, 3-MA was only able to partially prevent the degradation of p62 induced by both treatments (Cl10 and Cl10 + PXT10), although being more efficient in counteracting the degradation of p62 caused by Cl10 alone.

Fig. 4 Levels of p62 on human C32 (**a**) and A375 (**b**) melanoma cells treated with Cl-IB-MECA (10 μM; Cl10; *grey bars*) or in combination with PXT (10 ng/mL; Cl10 + PXT; *grey bars*), after 24-h incubation, in the absence or in the presence of the autophagy inhibitor, 3-MA (2.5 mM, *grey hatched bars*). DMSO (final concentration of 0.1 % v/v) in DMEM-HG was used as vehicle (*white bars*) and LY294002 (50 μM, *black bars*) as a positive control for autophagy. Results of levels of p62 [optic density at 450(OD$_{450}$)/ng protein] are presented as mean ± SEM, $n = 12$ of 4 independent experiments. Significant differences (one-way ANOVA test, followed by the Student–Newman–Keuls post hoc test): $*p < 0.05$ versus vehicle; $***p < 0.001$ versus vehicle; $^{#}p < 0.05$ versus same treatment without 3-MA; $^{##}p < 0.01$ versus same condition in the absence of 3-MA; $^{$}p < 0.05$ versus LY294002; $^{φ}p < 0.05$ versus Cl10
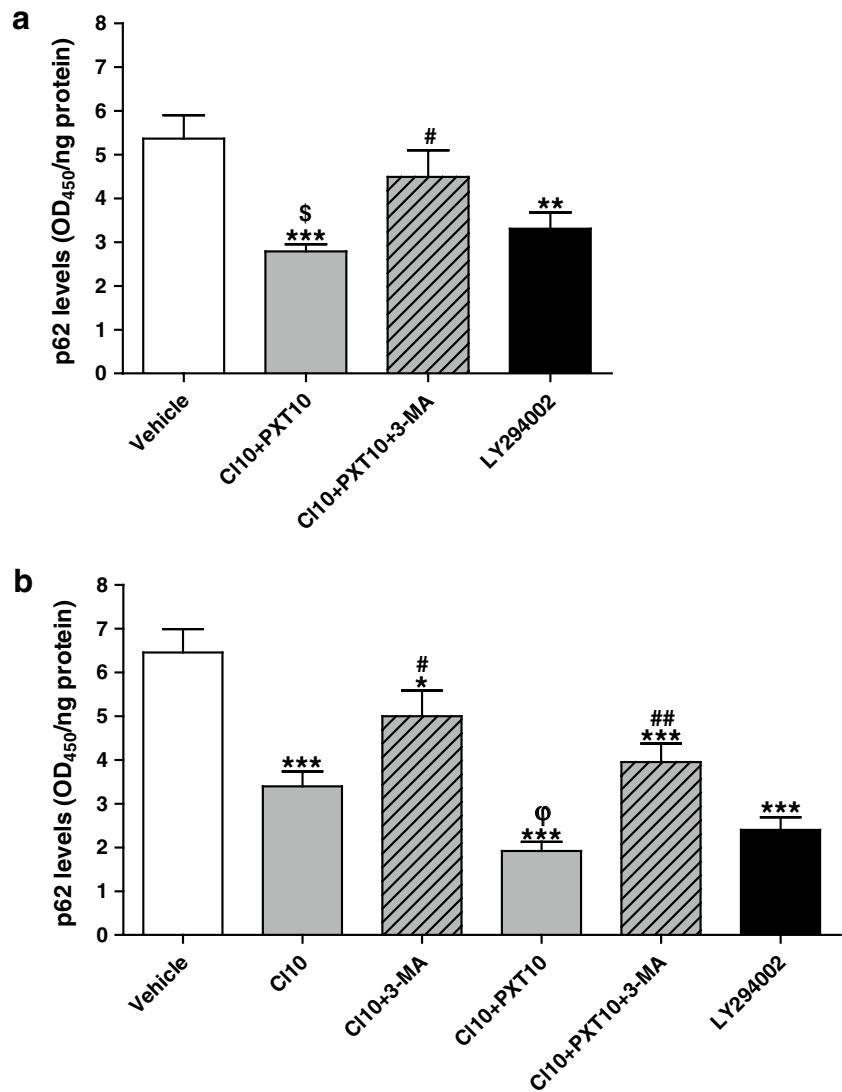
Reduction in mTOR levels is related to autophagic cell death activation triggered by Cl-IB-MECA in A375 cells and by Cl-IB-MECA with PXT in A375 and C32 melanoma cells

Evaluation of mTOR, a downstream effector of the PI3K/AKT signalling pathway that suppresses autophagy, was also performed by immunofluorescence, after cell treatments where autophagy occurs. As such, cells were incubated with Cl10, PXT10, and combination of Cl10 with PXT10 (Cl10 + PXT10), in the absence or in the presence of an autophagy inhibitor, 3-MA (2.5 mM), for 24 h, as described in the Methods section. LY294002 (50 μM) was used as a positive control for autophagy.

Images presented in Fig. 5 showed cells intensely stained (red) in conditions where there is no autophagy activation, as a result of high levels of mTOR protein in those conditions. C32 cells treated with Cl10 in combination with PXT10, and A375 cells treated with Cl10 and Cl10 in combination with PXT10 for 24 h, presented a decrease in mTOR expression revealed by a decrease in red fluorescence intensity. A similar low pattern of red fluorescence was also observed in cells, from both cell lines, incubated with the positive control for autophagy, after 24-h incubation (Fig. 5). These results suggest the involvement of the mTOR pathway on autophagic melanoma cell death induced by Cl10 on A375 cells and by Cl10 in combination with PXT10 on both human melanoma cell lines.

Mitotic catastrophe is induced by caspase-dependent and caspase-independent mechanisms triggered by PXT and Cl-IB-MECA in combination with PXT

Since PXT-induced cell death is solely related with apoptosis, only when combined with Cl-IB-MECA autophagy was seen, efforts were also made in order to further explore
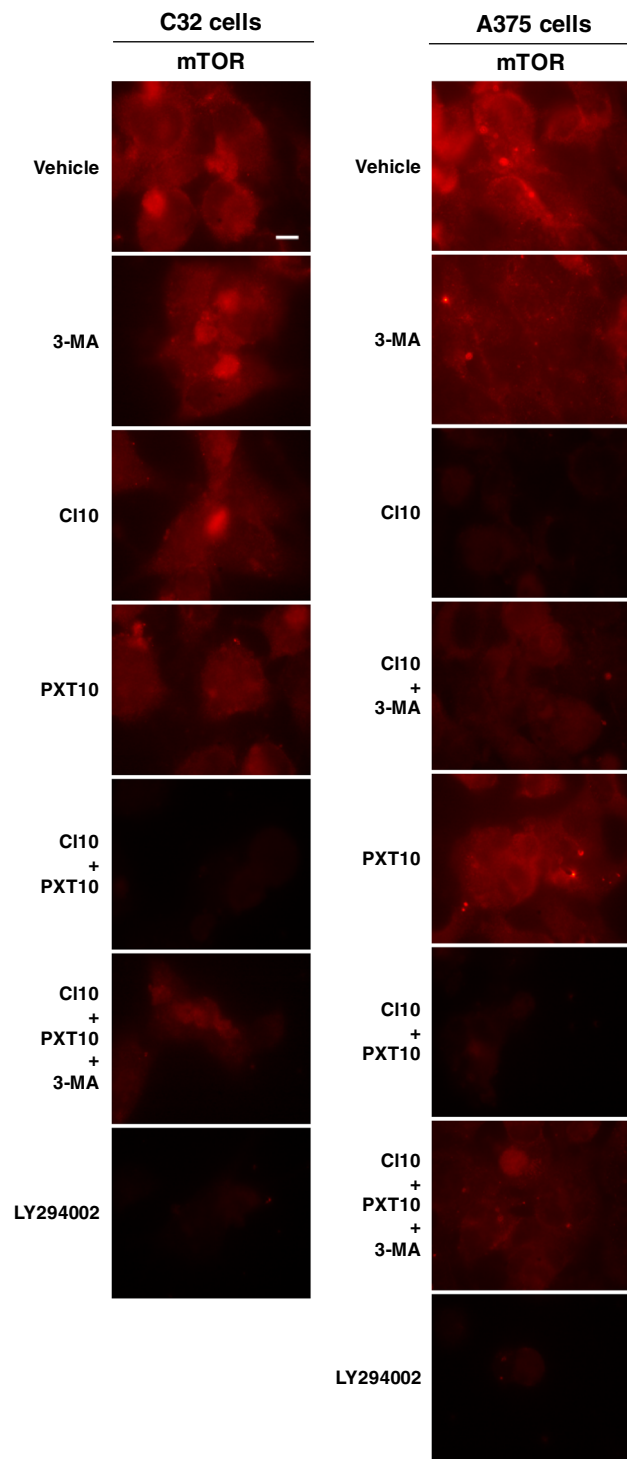
Fig. 5 Levels of mTOR on melanoma cells treated with Cl-IB-MECA (10 μM; Cl10) and/or with PXT (10 ng/mL; PXT10), after 24-h incubation, in the absence or in the presence of the autophagy inhibitor, 3-MA (2.5 mM). DMSO (final concentration of 0.1 % v/v) in DMEM-HG was used as vehicle and LY294002 (50 μM) as a positive control for autophagy. Representative photographs of C32 and A375 cells after mTOR (*red staining*) of $n = 4$ independent experiments. *Scale bar* 10 μm

the mechanisms of PTX-induced apoptosis. Images from PXT treatments labelled with Hoechst 33258 highlighted the occurrence of micro- and multinucleated cells, typical of MC (Fig. 5). To confirm the occurrence of MC, effects of PXT alone or in combination with Cl-IB-MECA on microtubule cytoskeleton (alpha-tubulin displayed in red) disruption were also examined by immunofluorescence. Human C32 and A375 melanoma cells were treated with Cl10, PXT10, and with the combination Cl10 + PXT10, in the absence or in the presence of a caspase inhibitor (Ac-DEVD-CHO, 50 μM), for 48 h (Fig. 6; Table 1). The vehicle and Cl10 alone showed typical radial and diffuse microtubule arrays (red alpha-tubulin) and normally shaped nuclei (blue) in both melanoma cell lines (Fig. 6), with similar MC/normal nuclei ratios (Table 1).

Red immunofluorescence staining showed that cell treatment with PXT (alone or in combination) disrupted microtubule networks in both melanoma cell lines (white arrows, Fig. 6). Furthermore, this effect was accompanied by the formation of micro- and multinucleated cells (blue stained nuclei, Fig. 6), morphological features associated with MC. The occurrence of such features was more significant when both cell lines were treated with Cl10 + PXT10 (Table 1). Moreover, the caspase inhibitor (Ac-DEVD-CHO) completely blocked the PXT-induced MC (Fig. 6; Table 1) but only partially prevent the effect caused by Cl10 + PXT10 (Fig. 6; Table 1). Taken together these results suggest that PXT10 causes MC by a caspase-dependent mechanism and when in combination with Cl10 causes MC by both caspase-dependent and caspase-independent mechanisms.

Enhanced cell death (LDH leakage assay) caused by PXT alone in A375 melanoma cells was completely prevented by NAC and significantly attenuated by this powerful antioxidant when cells were treated with Cl10 in combination with PXT10 (Table 2). These data suggest that PXT can induce reactive oxygen species (ROS) generation, leading to its cytotoxicity.

Discussion

The present study provides evidence that Cl-IB-MECA in combination with PXT can induce mTOR-dependent autophagic cell death, and caspase-dependent and or/independent MC-related apoptosis, on human C32 and A375 melanoma cells (Fig. 7). The activation of these mechanisms may prove to be useful towards the therapy of one of the most deadly and therapeutically challenging cancers, the melanoma.

We previously showed that Cl-IB-MECA and PXT, alone or in combination, caused caspase-dependent apoptosis on C32 cells, as a cytotoxic mechanism (Soares et al.
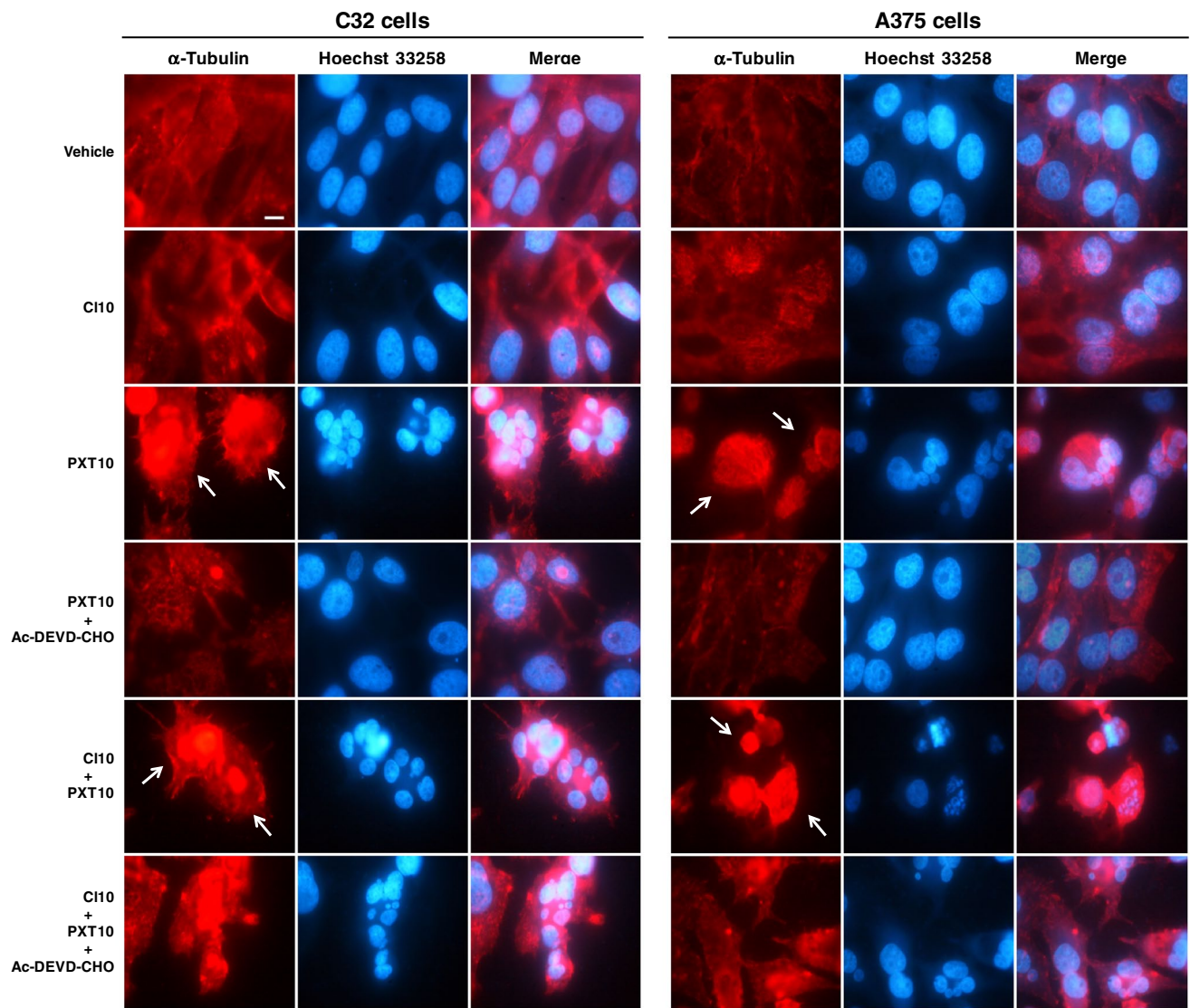
Fig. 6 Evaluation of mitotic catastrophe induced by PXT (10 ng/mL, PXT10) and/or by Cl-IB-MECA (10 µM, Cl10), after 48-h incubation, in the absence or in the presence of the caspase inhibitor, Ac-DEVD-CHO (50 µM). DMSO (final concentration of 0.1 % v/v) in 2013). DMEM-HG was used as vehicle. Representative photographs of C32 and A375 cells after alpha-tubulin (*red*) and nuclei (*blue*) staining (*n* = 4 independent experiments). *Scale bar* 10 µm. *Arrows* indicate microtubules disruption (*red*)

2013). In fact, we demonstrated that the activity of caspase 3 (and also 8 and 9) was augmented after cell treatment with this combination (Soares et al. 2013). However, it is of great interest to examine the efficacy of the proposed therapeutic strategy on other melanoma cellular models and the other possible mechanisms involved. As such, we used the lowest concentrations of Cl-IB-MECA (10 µM, Cl10) and PXT (10 ng/mL, PXT10) tested in the previous work, and the combination of both, on human C32 and A375 metastatic melanoma cells. These are clinically relevant concentrations since Cl-IB-MECA showed no serious drug-related adverse effects or dose-limiting toxicities, and good oral bioavailability in clinical trials (Stemmer et al. 2013), and

PXT concentrations found in plasma cancer patients were 2.6 times higher than the one used in this study (Rodriguez et al. 2012). Cytotoxic effects were measured using several assays, MTT reduction and NR uptake assays and also the LDH leakage assay, to increase the reliability of the results obtained. Results now presented are the first demonstration that Cl-IB-MECA in combination with PXT is also an effective cytotoxicity inducer in another melanoma cellular model: A375 cells. Each cell line seems to have different sensibility towards Cl10, whereas with PXT10 or the combination of drugs, the effects seem to be similar. In fact, C32 cells when incubated with Cl10 have their NR uptake ability strongly compromised, whereas A375 cells

Table 1 Quantification of mitotic catastrophe induced by PXT (10 ng/mL, PXT10) and/or by Cl-IB-MECA (10 μM, Cl10), after 48-h incubation, in the absence or in the presence of the caspase inhibitor, Ac-DEVD-CHO (50 μM)

48 h	Nuclei ratio (mitotic catastrophe/normal) (mean ± SEM)	
	C32 cells	A375 cells
Vehicle	0.23 ± 0.02	0.19 ± 0.04
Cl10	0.22 ± 0.01	0.23 ± 0.03
PXT10	1.94 ± 0.03***	1.27 ± 0.01***
PXT10 + Ac-DEVD-CHO	0.22 ± 0.02###	0.19 ± 0.02###
Cl10 + PXT10	1.69 ± 0.01***,††	3.70 ± 0.4***,†††
Cl10 + PXT10 + Ac-DEVD-CHO	0.53 ± 0.03***,###	0.94 ± 0.04***,###

DMSO (final concentration of 0.1 % v/v) in DMEM-HG was used as vehicle. Results of nuclei ratio (mitotic catastrophe/normal) are presented as mean ± SEM, $n = 10$ random fields of 4 independent experiments

Significant differences (one-way ANOVA test, followed by the Student–Newman–Keuls post hoc test): *** $p < 0.001$ versus vehicle; ### $p < 0.001$ versus same condition in the absence of Ac-DEVD-CHO; †† $p < 0.01$ versus PXT10; ††† $p < 0.001$ versus PXT10

Table 2 Effect of NAC (1 mM) on the cytotoxicity caused by Cl-IB-MECA (10 μM; Cl10) and/or PXT (10 ng/mL; PXT10) on human A375 melanoma cells, after 48-h incubation

48 h	LDH leakage (% from total LDH)	
	(−) NAC (mean ± SEM)	(+) NAC (mean ± SEM)
Vehicle	7.07 ± 0.42	6.83 ± 0.46
Cl10	18.58 ± 0.74	17.97 ± 0.98
PXT10	14.82 ± 0.53	$7.79 \pm 0.95$$$$
Cl10 + PXT10	35.82 ± 1.16	$32.39 \pm 1.17$$

DMSO (final concentration of 0.1 % v/v) in DMEM-HG was used as vehicle. Results of LDH leakage (% of total LDH) are presented as mean ± SEM, $n = 9$ of 3 independent experiments

Significant differences (one-way ANOVA test, followed by the Student–Newman–Keuls post hoc test): $ $p < 0.05$ versus same condition in the absence of NAC; $$$ $p < 0.001$ versus same condition in the absence of NAC. Other significant differences were similar to Fig. 2b

show alterations in their cellular membrane integrity (LDH assay) in the same condition. Of relevance, the combination has the same cytotoxic profile in both cell lines, showing higher clinical potential.

The combination of Cl-IB-MECA with PXT was reported to induce apoptosis in C32 melanoma cells (Soares et al. 2013). However, other mechanisms of cell death are most definitively involved since, in this study, the caspase inhibitor only prevented approximately 10 % of the cytotoxic effects described. In the present study, we tested the combination of Cl10 with PXT10 in the presence of Ac-DEVD-CHO (a caspase inhibitor) and/or 3-MA (an autophagy inhibitor) as the our used combination seems to largely impair lysosomal functions. The LDH leakage assay was chosen to assess cell death since permanent cell membrane rupture is expected to occur at a later stage (Weyermann et al. 2005), allowing us to better distinguish between overall cytotoxicity from specific organelle damage.

Results demonstrated that Cl10 did not induce any type of cell death on C32 cells, in opposition to its effect upon A375 cells where cell death occurs exclusively mediated by autophagy. To the best of our knowledge, it is the first time that Cl10 is reported to induce autophagy in melanoma cells. Autophagy induction is currently taken to represent a novel therapeutic target for apoptosis-resistant cancers (Tsujimoto and Shimizu 2005).

The discrepancy between C32 and A375 cells concerning their susceptibility to Cl10 could be, in part, related to donator's gender, since C32 and A375 cells were collected from male to female human donators, respectively. This possibility is in agreement with the different metastatic spread patterns found on gender of patients with metastatic melanoma (Mervic 2012). This difference, however, does not alter the cytotoxic response towards PXT10. The present work provides evidence that PXT10 alone elicits exclusively caspase-dependent apoptosis on both melanoma cell lines. Indeed, PXT is a well-established mitotic spindle anticancer drug reported to induce apoptosis in many types of cancer (Steed and Sawyer 2007), including melanoma (Wang et al. 2003).

Importantly, the present work demonstrates that besides apoptosis, Cl10 in combination with PXT10 also induces autophagy, causing cell death in both melanoma cell lines (Fig. 7). Indeed, when caspase-dependent apoptosis or autophagy was inhibited, cell death was not completely prevented. Activation of these two types of cell death has also been reported to occur on ME1402 and WM1158 melanoma cells after treatment with a new binuclear palladacycle complex (Aliwaini et al. 2013). Our results also indicate that for C32 cells, autophagy represents the main cell death mechanism of the drug combination, contrary to what happens in A375 cells where apoptosis and autophagy contribute at a similar extent (Fig. 7). Moreover, the simultaneous addition of a caspase and an autophagy inhibitor was not able to completely block cell death caused by Cl10 + PXT10 on A375 cells. Although Ac-DEVD-CHO is referred as a selective caspase 3/7 inhibitor, the concentration used in the present study also blocks caspase-6 (Mintzer et al. 2012), preventing all effector caspases activation. Thus, the possibility of other effector caspases being active can be discarded and necrosis (Jain et al. 2013) can be suggested as the probable mechanism through which Cl10 in combination with PXT10 induced the non-autophagic and non-apoptotic A375 cell death.

Fig. 7 Proposed signalling pathways showing the induction of autophagy through mTOR activation, with autophagosome-lysosome fusion, by the combination of Cl-IB-MECA and PXT on human C32 and A375 melanoma cell lines. This combination decreases mTOR levels, leading to the sequestration of cargo (autophagosomes) and fusion with lysosomes, leading to autophagy. Moreover, Cl-IB-MECA with PXT causes micro- and multinucleation, characteristic of mitotic catastrophe (MC), through caspase-dependent and/or independent mechanisms, followed by apoptosis. *Red boxes* represent selective inhibitors. *Dashed arrow* represents an indirect pathway
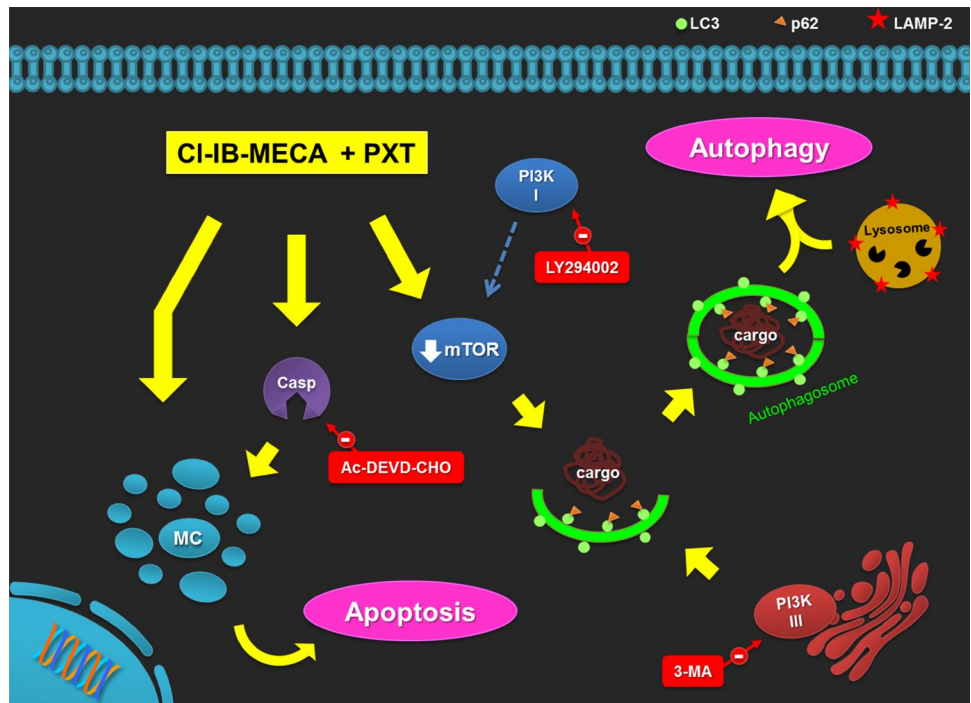
As autophagy seems to be responsible for most of the C32 and A375 cell death induced by treatment with Cl-IB-MECA and PXT, other characteristic markers of the autophagic process were also analysed to confirm this hypothesis: formation of a double-membrane vacuole (autophagosome) and subsequent fusion with lysosome (autolysosome) (Kung et al. 2011), and degradation of the intracellular levels of p62 (also called SQSTM1 in humans) (Puissant et al. 2012).

We detected a relative high accumulation of autophagosomes (through MDC staining) and their co-localization with lysosomes (through RFP fused lysosomal signal via LAMP 1 protein expression), after treatment of A375 cells with Cl10 and of both cell lines with Cl10 and PXT10. Moreover, 3-MA inhibited the formation of autophagosomes in these conditions. A class III and a class I PI3K inhibitor, 3-MA and LY294002, respectively, were used to inhibit and activate the autophagy process (Liu et al. 2013).

The understanding that p62 binds directly to LC3 (recruited to autophagosomal membranes) resulting in specific degradation of this protein by autophagy makes p62 a valuable and largely used marker for autophagy (Komatsu et al. 2012), since interaction of p62 with LC3 is required for autophagy-mediated elimination of unfolded ubiquitinated long-half-life proteins and non-ubiquitinated substrates (Puissant et al. 2012). As expected, a decrease in p62 levels from C32 cells treated with Cl10 and PXT10, and A375 cells treated with Cl10 alone or in combination with PXT10, was observed in the conditions where autophagosome formation was visualized through fluorescence

microscopy. The 3-MA inhibitor was able to completely prevent the autophagic flux in C32 cells, and almost total blockade was achieved on A375 cells. Overall, these findings corroborate those obtained with the LDH leakage assay and confirm that induction of autophagy is, in fact, a cytotoxic mechanism in our conditions. Although there is a controversy whether autophagy activation promotes defensive or destructive roles in response to cancer therapy (White and DiPaola 2009), emerging evidence indicates that several cytotoxic agents are autophagic inducers of melanoma cell death (Tomic et al. 2011; Nicolau-Galmes et al. 2011).

Even though mechanisms of autophagy regulation are not completely understood, evidences have shown that mTOR, a protein kinase member of the PI3K-related family, which is involved in cell proliferation, plays a major role in controlling autophagy activation (Mizushima 2007). Moreover, targeting mTOR is considered as a promising target for cancer therapy, as dysregulation of mTOR signalling is present in a variety of human malignancies (Meric-Bernstam and Gonzalez-Angulo 2009). In agreement with these facts, we found an inverse correlation between levels of mTOR and autophagy activation. Levels of mTOR were significantly decreased in C32 cells treated with Cl10 + PXT10 and A375 cells treated with Cl10 and Cl10 + PXT10, conditions where autophagy was previously shown to occur. Autophagy was found to be regulated through the suppression of mTOR expression (Quidville et al. 2013; Wang et al. 2013). Considering current knowledge, it is conceivable that these cell treatments

inhibit class I PI3K and/or AKT, leading to downregulation of mTOR expression, since the effect was similar to that achieved with the LY294002 (Fig. 7).

Overall, it seems that Cl-IB-MECA is a more potent inducer of autophagic cell death than PXT, since the latter, when alone, did not show any signs of autophagy activation.

In fact, we found that PXT alone was fully linked to induction of apoptosis. This anticancer drug has already shown to be efficient in the treatment of different cancers, including melanoma (Wang et al. 2003). Unfortunately, the molecular mechanisms involved in PXT-induced apoptosis are poorly understood (Bhalla 2003). We characterized the microtubules network in C32 and A375 cells after treatment with PXT10 and Cl10 + PXT10 and found that PXT alone or in combination with Cl-IB-MECA strongly disrupted microtubules network and induced micro- and multinucleation, both hallmarks of MC (Fig. 7). Moreover, we demonstrated that prevention of caspase activation completely suppressed PXT10-induced MC signals in opposition to what was observed for the combination of Cl10 with PXT10, where MC was not totally prevented in either melanoma cell line. These facts indicate that PXT10 induced caspase-dependent MC in C32 and A375 cells; however, caspase-independent phenomena is also involved in the MC elicited by Cl10 + PXT10 in both cell lines. Although caspase-dependent MC is being suggested as a special case of apoptosis (Castedo et al. 2004a, b), MC cell death through caspase-dependent and caspase-independent mechanisms was also reported (Mansilla et al. 2006), corroborating our present results.

It is currently accepted that ROS generation can trigger MC (Hung et al. 2013). This possibility was checked by evaluating A375 cell death (LDH leakage assay) caused by PXT, alone or in combination with Cl-IB-MECA, in the presence of NAC. In our previous study (Soares et al. 2013), this powerful antioxidant prevented cytotoxicity on C32 cells treated with PXT10. In the present study, we found that NAC completely prevent PXT10-induced A375 cell death, suggesting that PXT induces ROS generation, which may cause MC cell death. ROS-dependent apoptosis caused by PXT has been previously described to occur in A375 cells (Selimovic et al. 2008). Interestingly, NAC was able to only slightly attenuate cytotoxicity elicited by the combination of Cl10 + PXT10, on A375 cells (Fig. 7).

In summary, the present study provides evidence that human C32 and A375 melanoma cells treated with Cl-IB-MECA and PXT undergo cell death by autophagy and MC-induced apoptosis (Fig. 7). We believe that the induction of autophagy in these cellular models, where cells are also undergoing apoptosis, provides appealing mechanisms concerning melanoma chemotherapy, since it drives more melanoma cells to die. Indeed, recently induction of autophagy was considered a very important cell death

mechanism when in combination with other conventional anti-melanoma therapies (Liu et al. 2013). The combination of Cl-IB-MECA and PXT seems, therefore, to be an attractive chemotherapeutic approach to melanoma because Cl-IB-MECA seems to largely improve the effectiveness of PXT by contributing to activate other forms of cell death (Fig. 7), increasing overall melanoma cells cytotoxicity and lowering PXT chemotherapy resistance.

Conflict of interest We declare that we have no conflict of interest in relation to this article.

References

Aliwaini S, Swarts AJ, Blanckenberg A, Mapolie S, Prince S (2013) A novel binuclear palladacycle complex inhibits melanoma growth in vitro and in vivo through apoptosis and autophagy. Biochem Pharmacol 86(12):1650–1663

Bhalla KN (2003) Microtubule-targeted anticancer agents and apoptosis. Oncogene 22(56):9075–9086

Biederbick A, Kern HF, Elsasser HP (1995) Monodansylcadaverine (MDC) is a specific in vivo marker for autophagic vacuoles. Eur J Cell Biol 66(1):3–14

Castedo M, Perfettini JL, Roumier T, Andreau K, Medema R, Kroemer G (2004a) Cell death by mitotic catastrophe: a molecular definition. Oncogene 23(16):2825–2837

Castedo M, Perfettini JL, Roumier T, Valent A, Raslova H, Yakushijin K, Horne D, Feunteun J, Lenoir G, Medema R, Vainchenker W, Kroemer G (2004b) Mitotic catastrophe constitutes a special case of apoptosis whose suppression entails aneuploidy. Oncogene 23(25):4362–4370

Dai DL, Martinka M, Li G (2005) Prognostic significance of activated Akt expression in melanoma: a clinicopathologic study of 292 cases. J Clin Oncol 23(7):1473–1482

de Souza CF, Morais AS, Jasiulionis MG (2012) Biomarkers as key contributors in treating malignant melanoma metastases. Dermatol Res Pract 2012:156068

Elmore S (2007) Apoptosis: a review of programmed cell death. Toxicol Pathol 35(4):495–516

Fulda S, Debatin KM (2006) Extrinsic versus intrinsic apoptosis pathways in anticancer chemotherapy. Oncogene 25(34):4798–4811

Gao S, Chen T, Choi MY, Liang Y, Xue J, Wong YS (2013) Cyanidin reverses cisplatin-induced apoptosis in HK-2 proximal tubular cells through inhibition of ROS-mediated DNA damage and modulation of the ERK and AKT pathways. Cancer Lett 333(1):36–46

Hanahan D, Weinberg RA (2011) Hallmarks of cancer: the next generation. Cell 144(5):646–674

Hengartner MO (2000) The biochemistry of apoptosis. Nature 407(6805):770–776

Hung JY, Wen CW, Hsu YL, Lin ES, Huang MS, Chen CY, Kuo PL (2013) Subamolide a induces mitotic catastrophe accompanied by apoptosis in human lung cancer cells. Evid Based Complement Altern Med 2013:828143

Jain MV, Paczulla AM, Klonisch T, Dimgba FN, Rao SB, Roberg K, Schweizer F, Lengerke C, Davoodpour P, Palicharla VR, Maddika S, Los M (2013) Interconnections between apoptotic, autophagic and necrotic pathways: implications for cancer therapy development. J Cell Mol Med 17(1):12–29

Jemal A, Siegel R, Xu J, Ward E (2010) Cancer statistics, 2010. CA Cancer J Clin 60(5):277–300

Jung CH, Ro SH, Cao J, Otto NM, Kim DH (2010) mTOR regulation of autophagy. FEBS Lett 584(7):1287–1295

Kihara A, Kabeya Y, Ohsumi Y, Yoshimori T (2001) Beclin-phosphatidylinositol 3-kinase complex functions at the trans-Golgi network. EMBO Rep 2(4):330–335

Komatsu M, Kageyama S, Ichimura Y (2012) p62/SQSTM1/A170: physiology and pathology. Pharmacol Res 66(6):457–462

Kung CP, Budina A, Balaburski G, Bergenstock MK, Murphy M (2011) Autophagy in tumor suppression and cancer therapy. Crit Rev Eukaryot Gene Expr 21(1):71–100

Liu H, He Z, Simon HU (2013) Targeting autophagy as a potential therapeutic approach for melanoma therapy. Semin Cancer Biol 23(5):352–360

LoPiccolo J, Blumenthal GM, Bernstein WB, Dennis PA (2008) Targeting the PI3K/Akt/mTOR pathway: effective combinations and clinical considerations. Drug Resist Updates 11(1–2):32–50

Maiuri MC, Zalckvar E, Kimchi A, Kroemer G (2007) Self-eating and self-killing: crosstalk between autophagy and apoptosis. Nat Rev Mol Cell Biol 8(9):741–752

Mansilla S, Priebe W, Portugal J (2006) Mitotic catastrophe results in cell death by caspase-dependent and caspase-independent mechanisms. Cell Cycle 5(1):53–60

Martins JB, Bastos Mde L, Carvalho F, Capela JP (2013) Differential effects of methyl-4-phenylpyridinium ion, rotenone, and paraquat on differentiated SH-SY5Y cells. J Toxicol 2013:347312

Meric-Bernstam F, Gonzalez-Angulo AM (2009) Targeting the mTOR signaling network for cancer therapy. J Clin Oncol 27(13):2278–2287

Mervic L (2012) Time course and pattern of metastasis of cutaneous melanoma differ between men and women. PLoS ONE 7(3):e32955

Mintzer R, Ramaswamy S, Shah K, Hannoush RN, Pozniak CD, Cohen F, Zhao X, Plise E, Lewcock JW, Heise CE (2012) A whole cell assay to measure caspase-6 activity by detecting cleavage of lamin A/C. PLoS ONE 7(1):e30376

Mizushima N (2007) Autophagy: process and function. Genes Dev 21(22):2861–2873

Mosmann T (1983) Rapid colorimetric assay for cellular growth and survival: application to proliferation and cytotoxicity assays. J Immunol Methods 65(1–2):55–63

Nicolau-Galmes F, Asumendi A, Alonso-Tejerina E, Perez-Yarza G, Jangi SM, Gardeazabal J, Arroyo-Berdugo Y, Careaga JM, Diaz-Ramon JL, Apraiz A, Boyano MD (2011) Terfenadine induces apoptosis and autophagy in melanoma cells through ROS-dependent and -independent mechanisms. Apoptosis 16(12):1253–1267

Puissant A, Fenouille N, Auberger P (2012) When autophagy meets cancer through p62/SQSTM1. Am J Cancer Res 2(4):397–413

Quidville V, Alsafadi S, Goubar A et al (2013) Targeting the deregulated spliceosome core machinery in cancer cells triggers mTOR blockade and autophagy. Cancer Res 73(7):2247–2258

Repetto G, del Peso A, Zurita JL (2008) Neutral red uptake assay for the estimation of cell viability/cytotoxicity. Nat Protoc 3(7):1125–1131

Rodriguez J, Contento AM, Castaneda G, Munoz L, Berciano MA (2012) Determination of morphine, codeine, and paclitaxel in human serum and plasma by micellar electrokinetic chromatography. J Sep Sci 35(17):2297–2306

Saiki S, Sasasawa Y, Imamichi Y, Kawajiri S, Fujimaki T, Tanida I, Kobayashi H, Sato F, Sato S, Ishikawa K, Imoto M, Hattori N (2011) Caffeine induces apoptosis by enhancement of autophagy via PI3K/Akt/mTOR/p70S6K inhibition. Autophagy 7(2):176–187

Santoni M, Amantini C, Morelli MB, Liberati S, Farfariello V, Nabissi M, Bonfili L, Eleuteri AM, Mozzicafreddo M, Burattini L, Berardi R, Cascinu S, Santoni G (2013) Pazopanib and sunitinib trigger autophagic and non-autophagic death of bladder tumour cells. Br J Cancer 109(4):1040–1050

Selimovic D, Hassan M, Haikel Y, Hengge UR (2008) Taxol-induced mitochondrial stress in melanoma cells is mediated by activation of c-Jun N-terminal kinase (JNK) and p38 pathways via uncoupling protein 2. Cell Signal 20(2):311–322

Shen S, Kepp O, Michaud M, Martins I, Minoux H, Metivier D, Maiuri MC, Kroemer RT, Kroemer G (2011) Association and dissociation of autophagy, apoptosis and necrosis by systematic chemical study. Oncogene 30(45):4544–4556

Soares AS, Costa VM, Diniz C, Fresco P (2013) Potentiation of cytotoxicity of paclitaxel in combination with Cl-IB-MECA in human C32 metastatic melanoma cells: a new possible therapeutic strategy for melanoma. Biomed Pharmacother 67(8):777–789

Soengas MS, Lowe SW (2003) Apoptosis and melanoma chemoresistance. Oncogene 22(20):3138–3151

Steed H, Sawyer MB (2007) Pharmacology, pharmacokinetics and pharmacogenomics of paclitaxel. Pharmacogenomics 8(7):803–815

Stemmer SM, Benjaminov O, Medalia G, Ciuraru NB, Silverman MH, Bar-Yehuda S, Fishman S, Harpaz Z, Farbstein M, Cohen S, Patoka R, Singer B, Kerns WD, Fishman P (2013) CF102 for the treatment of hepatocellular carcinoma: a phase I/II, open-label, dose-escalation study. Oncologist 18(1):25–26

Tawbi HA, Kirkwood JM (2007) Management of metastatic melanoma. Semin Oncol 34(6):532–545

Tomic T, Botton T, Cerezo M, Robert G, Luciano F, Puissant A, Gounon P, Allegra M, Bertolotto C, Bereder JM, Tartare-Deckert S, Bahadoran P, Auberger P, Ballotti R, Rocchi S (2011) Metformin inhibits melanoma development through autophagy and apoptosis mechanisms. Cell Death Dis 2:e199

Tsujimoto Y, Shimizu S (2005) Another way to die: autophagic programmed cell death. Cell Death Differ 12(Suppl 2):1528–1534

Vakifahmetoglu H, Olsson M, Zhivotovsky B (2008) Death through a tragedy: mitotic catastrophe. Cell Death Differ 15(7):1153–1162

Wang F, Cao Y, Zhao W, Liu H, Fu Z, Han R (2003) Taxol inhibits melanoma metastases through apoptosis induction, angiogenesis inhibition, and restoration of E-cadherin and nm23 expression. J Pharmacol Sci 93(2):197–203

Wang S, Xia P, Ye B, Huang G, Liu J, Fan Z (2013) Transient activation of autophagy via Sox2-mediated suppression of mTOR is an important early step in reprogramming to pluripotency. Cell Stem Cell 13(5):617–625

Weyermann J, Lochmann D, Zimmer A (2005) A practical note on the use of cytotoxicity assays. Int J Pharm 288(2):369–376

White E, DiPaola RS (2009) The double-edged sword of autophagy modulation in cancer. Clin Cancer Res 15(17):5308–5316

Xing C, Zhu B, Liu H, Yao H, Zhang L (2008) Class I phosphatidylinositol 3-kinase inhibitor LY294002 activates autophagy and induces apoptosis through p53 pathway in gastric cancer cell line SGC7901. Acta Biochim Biophys Sin 40(3):194–201